

Article

Comparative Analysis of Boron-Al Metal Matix Composite and Aluminum Alloy in Enhancing Dynamic Performance of Vertical-Axis Wind Turbine

Abhishek Agarwal ^{1,*}  and Linda Mthembu ² 

¹ Department of Mechanical Engineering, College of Science and Technology, Royal University of Bhutan, Phuentsholing 21101, Bhutan

² Department of Mechanical Engineering, University of South Africa, Science Campus, Private Bag X6, Florida 1710, South Africa; mthemls@unisa.ac.za

* Correspondence: agarwala.cst@rub.edu.bt

Abstract: This study aims to assess the dynamic performance of the vertical-axis wind turbine (VAWT) with the help of conventional aluminum (Al) and the boron Al metal matrix composite (MMC). The simulations were conducted using ANSYS software and involved natural frequencies, mode shapes, a mass participation factor, and Campbell plots. The results of static structural analysis show that the boron Al MMC is vastly superior to the aluminum alloy because there is a 65% reduction of equivalent stress with a 70% reduction of deformation compared to the aluminum alloy. These results show that boron Al MMC can withstand higher loads with lesser stress; the structure remains compact and rigid in its working conditions. From the findings, it can be ascertained that employing boron Al MMC improves VAWT power, efficiency, and robustness. However, the critical speed that was established in the dynamic analysis of boron Al MMC requires extraordinary control and the use of dampening systems, thereby avoiding resonance. Overall, boron Al MMC contributes to significant enhancements in the VAWTs' mechanical and operational characteristics; however, the material's complete potential can be achieved only with proper maintenance and employing the correct damping techniques. Information about these two materials will allow for a better understanding of their comparative efficacy and their potential application in the further development of VAWTs.

Keywords: modal analysis; vertical-axis wind turbine (VAWT); boron aluminum metal matrix composite; dynamic characteristics; FEA analysis; structural optimization; Campbell diagrams



Citation: Agarwal, A.; Mthembu, L. Comparative Analysis of Boron-Al Metal Matix Composite and Aluminum Alloy in Enhancing Dynamic Performance of Vertical-Axis Wind Turbine. *Processes* **2024**, *12*, 2288. <https://doi.org/10.3390/pr12102288>

Academic Editors: Zhou Li and Yao Lu

Received: 12 July 2024

Revised: 13 August 2024

Accepted: 14 October 2024

Published: 18 October 2024



Copyright: © 2024 by the authors. Licensee MDPI, Basel, Switzerland. This article is an open access article distributed under the terms and conditions of the Creative Commons Attribution (CC BY) license (<https://creativecommons.org/licenses/by/4.0/>).

1. Introduction

Wind turbines have become one of the most promising technologies for the alternative sourcing of energy in the search for renewable and sustainable energy. Turbines for the generation of electric power harness the kinetic energy of wind, and the process of doing so has undergone significant improvement over the years [1]. In the past, windmills were mainly used as mechanical appliances to turn machines like water pumps and mills used for grinding grains. They are, however, very central in producing power, especially in wind electricity production facilities which range across expansive regions in the world today [2]. Among the types of wind turbines, the vertical-axis wind turbine (VAWT) has received significant attention because of the characteristics of its structure and functionality. Compared with the horizontal-axis wind turbine (HAWT), all the main rotor shafts of the VAWT are arranged vertically, and the VAWT does not need to employ a yawing mechanism since it can receive the wind from every direction [3]. This attribute makes VAWTs particularly suitable for operation in urban areas and areas with turbulent wind patterns [4]. Nonetheless, VAWTs present certain challenges, where the major concern is the vibrations of the blades. The blades of a VAWT are typically long and very flexible, making them prone to dynamic responses. Due to these forces, the blades may vibrate, and if not

controlled, these vibrations can result in high fatigue loads, ultimately causing the turbine components to fail [5]. Therefore, it is necessary to study and reduce such vibrations if better efficiency and durability of VAWTs are to be achieved. More specifically, due to the nature of such rotor dynamics, such as the vibration characteristics, extensive analysis of VAWT dynamic characteristics should be conducted to eliminate resonant problems [6]. This phenomenon arises when the frequency of a turbine blade's vibrations matches the frequency of the external forces applied to it, significantly increasing the amplitude. This may lead to catastrophic failure; thus, it is vital to perform efficient vibration analysis and control techniques.

The importance of embarking upon these problems can be described in the following way: first of all, the potential increase in dynamic stability of VAWTs contributes to the creation of more reliable turbines with less frequent breakdowns and subsequent maintenance expenses; second, by optimizing the operation of VAWTs, the total renewable energy output of wind power can be improved, which is beneficial for a better and more reliable wind energy supply; third, controlling vibration problems can increase the suitability of VAWTs in operation under offshore and city conditions, which increases the prospects of renewable energy sources [7].

Metal matrix composites (MMCs) offer higher stiffness, improved strength-to-weight ratios, and lower densities, which are crucial for minimizing blade vibrations and enhancing turbine performance [8]. In this regard, the integration of some advanced materials can be seen as one of the ways of optimizing the dynamic properties of the VAWTs. This study is intended to explore the dynamic behaviors of VAWTs, with particular reference to MMCs. The intended study will also be aimed at investigating the theoretical explanation for blade vibrations, the steps involved in integrating MMCs, and the consequences of this practice. This work aims at enhancing the performance of VAWTs—and hence the promotion of renewable energy technologies—by presenting new methodologies for analysis and by providing empirical support to the proposed designs with the intent that improved VAWTs will become more widely utilized in the future.

Wind turbines are large machines that use the energy of wind through their mechanical parts to produce electricity [9]. Traditionally, the application of wind turbines was considered for the utilization of wind power in operating some sort of machinery, such as water pumps [10]. However, in the present era, they are mostly utilized for the generation of electricity in wind farms [11]. Fatigue load and vibration in vertical-axis wind turbines (VAWT) are rather sensitive, especially with blades of large and slender size. This has led to blade vibration being a major issue in the field. Therefore, in precluding the resonance that leads to an increase in amplitude and thus system failure, it is necessary to evaluate the vibration properties of wind turbines [12]. Several scientific publications have been devoted to this topic, and they analyze different aspects of VAWT dynamics and possible control methods.

1.1. Dynamics and Control of VAWT Blades

Mthembu et al. [13] found that the installation of VAWTs increased considerably in regions with limited space and unstable wind directions, due to the elimination of the yaw mechanism, which would otherwise be needed to adjust to changing wind directions. In their work, they conducted CFD analysis and stressed that VAWTs could be suitable for hydrogen production, while at the same time highlighting that design enhancement constituted a problematic area.

Basu et al. [14] studied the application of smart mass dampers for the enhancement of in-plane tower vibrations of the wind turbine. Their study showed a very precise numerical model of two horizontally placed multiple-tuned mass dampers. The possibility of employing an active tuned mass damper (ATMD) was considered as a viable solution to the problem of controlling vibrations in tower/nacelle constructions in real time. Performance tests of VAWTs were carried out by Agarwal A. [15], where the author undertook a CFD study to establish the torque produced at 10 m/s wind velocity. According to their research,

the authors concluded that there is a positive correlation between power production in VAWTs and the blades' height, as well as structural improvements; however, aerodynamics have been identified as a critical factor in the efficiency of VAWTs.

1.2. *Vibration Mitigation Techniques*

In the study by Brodersen et al. [16], the authors sought to reduce tower vibration via active tuned mass dampers (ATMD). The measurement of the effects of ATMD vibration control was the main area of concern of their study, and more so on a fixed offshore wind turbine. The control algorithm of the ATMD obtained the signal from both the movement of the tower and the speed of the damper; the tuning of the damper and control force frequencies was also conducted. Based on the HAWC2 finite element analysis, it was established that the ATMD outcomes reduced both transient and frequency responses, as opposed to other passive TMDs. Coudurier et al. [17] investigated the use of the tuned liquid column damper to reduce vibration in offshore wind turbines. They analyzed two control techniques: the passive coupled system and the semi-active control system. It was concluded from the results that TLCD semi-control was less effective than passive dampers in the reduction of vibration but effective only in cases where better control systems were required in dynamic applications.

1.3. *Advanced Modeling and Analysis*

Woude and Narasimhan [18] examined the vibration isolation technology in wind turbines to predict the behavior of wind turbines through finite element analysis, as proposed by the European Agency in 2020. As for the validation of the proposed strategy, the Bouc–Wen model was used, with the blades and turret modeled as structural parts of the vibration isolator [19]. In this study, the urgent need to develop more complex modeling approaches was underlined to improve the performance of the turbines. F. Geng et al. [20] contributed an enhanced computational modeling approach for the fatigue assessment of VAWTs. Their work quantified the effect of the VAWT's static and fatigue properties, certain parameters modeling, and the presence of structural defects on the fatigue response of the VAWT. Thus, a 25% reduction in fatigue life is found in VAWT, depending on the flaw sizes and location, showing the significance of structures on turbines.

1.4. *Innovative Control Methods*

Wen Fang et al. [21] outlined an SCPD control technique for intelligent blade control for trailing edge flaps in wind turbines. The proposed SCPD control algorithm exhibits a simple structure, a small computational volume, and high robustness; furthermore, it has good test results in terms of vibration suppression and probably has the flexibility to cope with complicated environments. Vishwaas Narasinh et al. [22] studied the effects of vibration on wind turbines with the help of analytical works. What they came up with was a prediction algorithm for generator speed loss and an indication of power loss based on vibrations. Their model, which comprises dimensionless vibration indices detrended by rotor RPM, offered an informative comparison of vibrations and their effects on turbine fuel efficiency. Jianwei Zhang et al. [23] introduced a new kind of bidirectional absorber-harvester (BAH) to deal with the bidirectional vibrations and, at the same time, convert the vibrations into electrical power. They found the best structure of BAH via numerical search techniques and showed that it may be used to improve the turbine performances in the worst conditions of wind–wave loading and the presence of yaw errors.

1.5. *Condition Monitoring and Predictive Maintenance*

The work of Francesco Castellani et al. [24] concerns the proposed method for predictive condition monitoring of WTG through actual industrial data. While using normal behavior modeling of the temperature patterns considering the data obtained from the SCADA system coupled with the support vector regression (SVR), the authors were able to pinpoint the trend of overheating in faulty turbines. This approach meant that faults

were noticed at a very early stage, and this enhanced the maintenance strategies of the turbines. Y. L. Dai et al. [25] worked on the effects of the fusion tip structure on wind turbine vibration behaviors. Such results of comparative trials of different tip designs indicated a considerable decrease in the vibration amplitude, thereby stressing the relevance of emerging designs for increased stability of turbines.

1.6. Material and Structural Optimization

In 2024, Peng Xue et al. [26] demonstrated a way to model and calculate the effect of materials and structural designs on weight reduction through a structurally optimized algorithm. Their framework showed that the blades made from Carbon Fiber Reinforced Plastics (CFRP) were 47% lighter, which is 1% lighter than those manufactured with Glass Fiber Reinforced Plastics (GFRP). Additionally, the corresponding structural parts were 44.8% lighter. In this study, the possibilities of weight loss and increased performance through material definition and structure modification were outlined. As mentioned by Agarwal et al. [27], the authors researched the application of metal matrix composites for the assessment of turbine blades. As evident in their discoveries, the incorporation of Al MMC material had the potential to decrease the stress on turbine vanes by 68.8%. From the dynamic simulation and analysis, it was concluded that the Al MMC turbine vane was found to have lower deformation compared to the structural steel, meaning that Al MMC materials would be appropriate for usage in turbine vane applications. Some of the critical issues discussed by A. Hamdan et al. [28] concerning VAWTs were the challenges related to the choice of the material for the bio-composite structure as well as the micro-energy harvesters. Ding et al. were able to bridge the existing knowledge by pinpointing gaps in the manufacturing process of bio-composite fibers, mainly in producing VAWTs, and they established that there is still a need to explore the mechanical properties of this material. Dayal Castro et al. [29] studied the mechanical behavior of natural composite VAWT blades manufactured with fique and epoxy using the finite element method. From the overall conclusion of their studies, they pointed out that fique–epoxy composites are effective alternatives to typical SFRP for handling air pressure loads, while also highlighting certain critical areas that correspond to the bonded union of plies [30].

These studies are available with significant implications in the renewable energy industry, collectively improving the modeling, control, material selection, and structure of VAWTs for better operation. While the literature contains numerous publications on the VAWT, there is still limited knowledge about the dynamic behavior of such turbines when using composite materials. Conventional materials like conventional aluminum have received considerable attention in the literature, while all formed material reinforcements, including the advanced metal matrix composites (MMCs) that include boron aluminum (boron Al) for its application in VAWTs, have not received adequate research attention. It is noteworthy that there is a deficiency in the current literature regarding comparative studies that quantify the dynamic behavior of VAWTs made from these materials, including natural frequencies, mode shapes, mass participation factors, and Campbell diagrams. Moreover, there are few comparative studies on the two materials—boron Al MMC and traditional aluminum—focusing on the vibration damping characteristics and strength of the structure under working load. Here, this research postulates that introducing MMC in the manufacturing of VAWT blades will tremendously enhance the dynamic performance in contrast to normal aluminum. Particularly, it is expected that the application of VAWTs with boron Al MMC blades will be more effective for improving the performance and durability of the turbines by decreasing the vibration level and avoiding resonance failure. Based on the above literature review, the following research questions were developed:

- What are the effects on the dynamic characteristics of VAWTs while using conventional materials and Metal matrix composite?
- What effects does the integration of boron Al MMC have on the general performance and durability of VAWTs?

- What basic factors should be considered while using boron Al MMC in the design and manufacturing of VAWTs to enhance efficiency and durability?

VAWTs are vital for efficient energy production; nevertheless, their performance is normally affected by vibration problems that reduce their performance and result in structural damage. There is also the possibility that new forms of material, such as the boron aluminum metal matrix composite material, may improve the dynamic performance of VAWTs, but the literature on the subject is scarce. This research seeks to partially fill this gap by determining the dynamic characteristics of VAWTs using the conventional aluminum and boron Al MMC materials for the blade by using the ANSYS simulation exercise. The objective is to find out if boron Al MMC can provide better dynamic performance and enhance the performance and reliability of VAWTs.

The present study aims to assess the dynamic behavior of VAWTs using regular aluminum and a new generation of Boron-Aluminum Metal Matrix Composites. Structural modeling and dynamic analysis will be conducted using ANSYS 18.1 simulation software. Among the results yielded by the dynamic analysis, natural frequencies, mode shapes, mass participation factors, and Campbell diagrams will be obtained. The Campbell diagram is significantly important in rotor dynamics as it helps in depicting the natural frequencies' relationship with the rotational speed. The graph of these frequencies against rotational speeds is useful in the identification of resonance situations whereby a system's natural frequency equals operational speed and is characterized by large vibrations and system failure [31,32]. This analysis helps maintain the steady and dependable characteristics of rotating machinery; by using it, engineers can avoid design parameters that will imply critical speeds, thus providing maximum protection. The objective of this study is to outline the factors that should be addressed in the utilization of the boron Al MMC material in VAWTs compared to normal aluminum material in terms of the improvement in turbine performance and durability.

2. Materials and Methods

The procedure for this study consists of a few important stages, which start with the modeling of VAWT and proceed to meshing, applying structural boundary conditions, and finally solving the dynamic analysis in ANSYS, as shown in Figure 1.

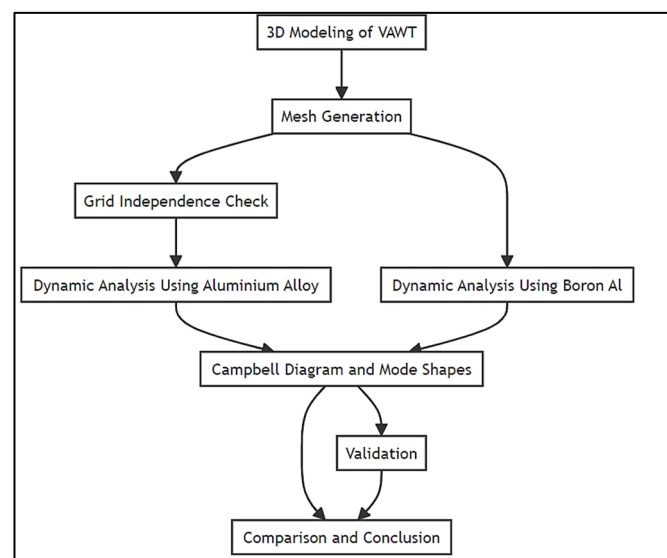


Figure 1. Flowchart of the FEA methodology.

2.1. CAD Modeling of Vertical Axis Wind Turbine

The geometry of the VAWT was created with the aid of Creo design software to generate the three-dimensional CAD model. Creo design software is used to model complex

3D CAD with high precision, hence ensuring a very accurate representation of the VAWT. The dimensions needed for the model are obtained from the literature [33]. Thus, the design maintains proportions with the standard dimensions for VAWTs, as provided in Table 1.

Table 1. Material properties used in VAWT [33].

Modules or Components	Parameter	Value with Unit
Straight Wind Blades or Airfoil	Chord Length	12 cm
	Blade Height	40 cm
Rotor Shaft	Shaft Length	48 cm
	Shaft Diameter	3.2 cm
Rotor Support Frame	Frame Diameter	36 cm
Bottom Base Support	Support I Diameter	30.5 cm
	Support II Diameter	23.6 cm

The 3D model of the VAWT is developed using the sketch, extrude, and revolve tool of the Creo parametric design software. The modeling process involves the development of airfoils as per NACA 0012, which are extruded to develop blades. Multiple copies of the blades are generated using a pattern tool, i.e., an axis pattern about the central shaft. In total, three blades are generated along with the base. The developed model was then transferred to ANSYS Design_modeler for additional processing. During this stage, the areas of hard edges, as well as any surface irregularities, were examined to ensure that these geometrical deviations would not impact the whole simulation model validity. The design, imported and cleaned, is shown in Figure 2 below.

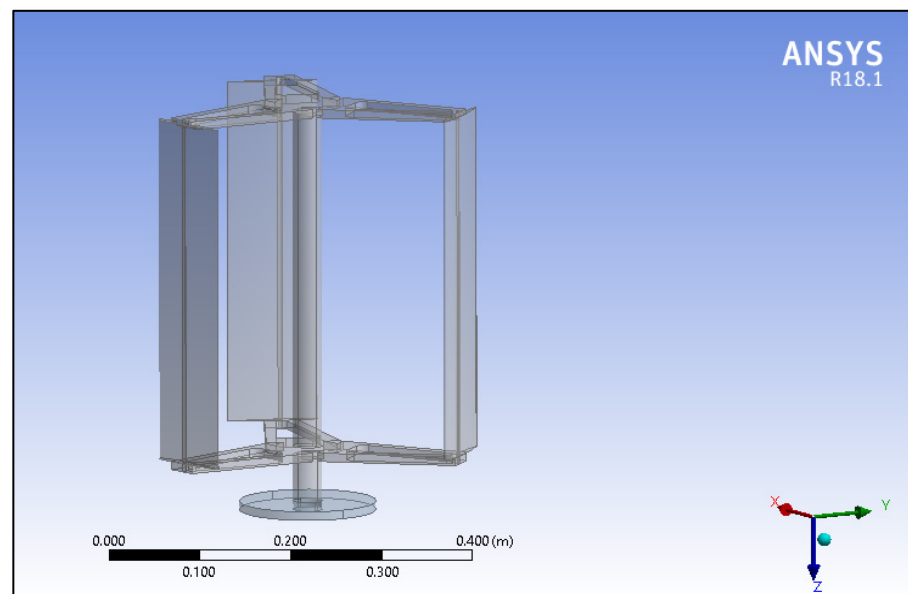


Figure 2. The imported CAD design of a vertical-axis wind turbine.

2.2. Material Properties

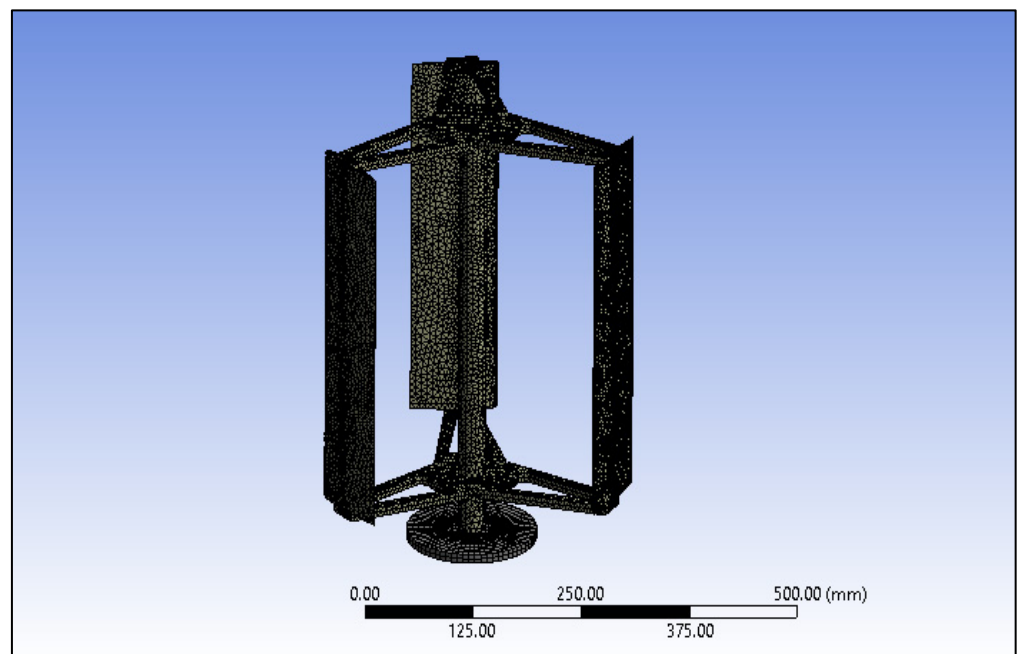
Two different materials were considered for the analysis: conventional aluminum alloy and advanced boron aluminum metal matrix composites. The boron Al MMC has boron carbide (B4C) and a base matrix of aluminum alloy. The boron fibers are used as the reinforcing phase due to their high hardness as well as lower density. The aluminum alloy used in the analysis is Al 6061-T6, which has 95.8% aluminum, and the remaining metals are magnesium, silicon, iron, copper, chromium, zinc, titanium, manganese, and other residuals. Material properties used in the simulation are shown in Table 2.

Table 2. Material properties used in VAWT [34].

Properties	Aluminum Alloy	Boron Al
Youngs Modulus (GPa)	71	235
Density (Kg/m ³)	2770	2700
Poisson's ratio	0.34	0.23

2.3. Meshing

The VAWT was then discretized for finite element analysis after modeling. Tetrahedral elements were chosen in light of complex curvatures, surface edges, and imperfections in the model. Tetrahedral elements can trace complex geometries more precisely due to their structure [35]. The tetrahedral element comprises 4 nodes with 3 DOFs/node. The growth rate for meshing is set to 1.2, smoothing is set to medium, and the transition ratio is set to 0.272. The meshing was set to fine relevance with normal inflation to ensure detailed and precise element distribution. The meshed model contained 94,247 elements and 163,900 nodes, as shown in Figure 3.

**Figure 3.** Meshed model of VAWT in ANSYS design_modeler.

2.4. Boundary Conditions

Structural loads and boundary conditions were applied to the meshed model. Fixed support was applied at the bottom of the VAWT, which is equivalent to the real-life constraints. Further, a rotational velocity of 50 rad/s was applied to the model to give an impression of the working conditions of the wind turbine. These boundary conditions are shown in Figure 4.

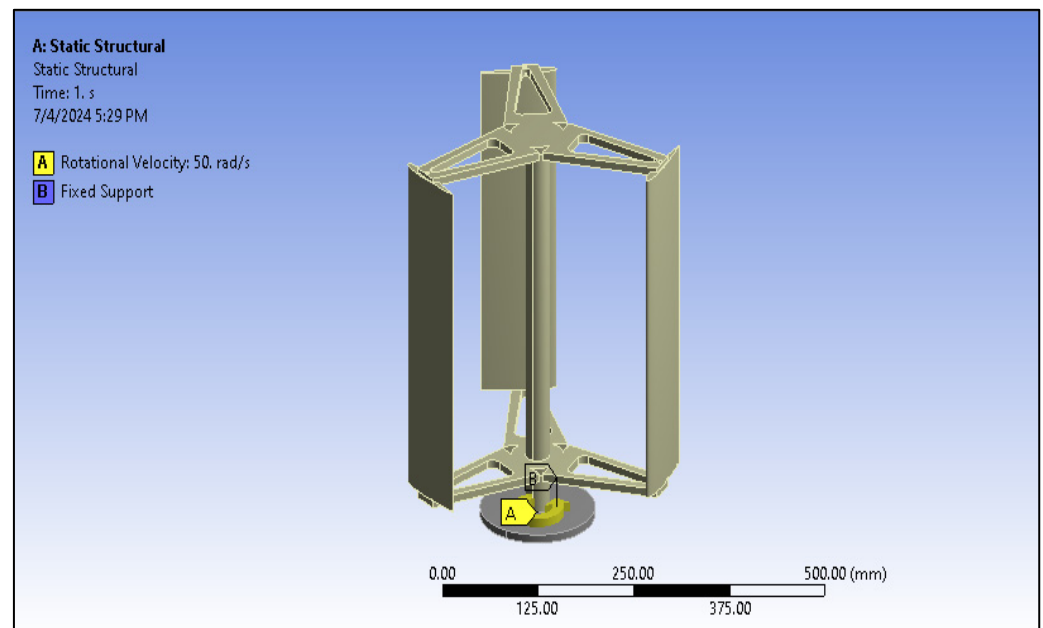


Figure 4. Applied boundary conditions to VAWT.

2.5. Simulation Scheme

The simulation process is conducted in the ANSYS workbench environment. The reason for choosing ANSYS is that it has very robust structural and dynamic analysis capabilities. The solver settings used in this analysis are the stiffness element formulation and the global element matrix formulation. These settings were chosen because this study focuses on representing the dynamic behavior of VAWT during its operational loadings. In-depth tools are available in ANSYS for checking geometric imperfections and running detail simulations. The tetrahedral element type is chosen as these are very good for models with complex curvatures and surface irregularities [36]. These ensure better mesh quality and accurate results. Fine relevance meshing ensures that even small details and surface imperfections are captured, leading to more accurate simulation results. Fixed support and rotational velocity boundary conditions reflect the real-world constraints and operational conditions of the VAWT, providing realistic and applicable results.

The above approach was chosen because it provides meticulous detail about the dynamic behavior of VAWTs made from different materials. The simulations were conducted with accurate modeling, fine meshing, selection of suitable material properties, and realistic boundary conditions to ensure that they are well matched to real-world situations. To the author's knowledge, most of the available literature lacks a comprehensive comparative study on traditional and advanced materials, including Boron-Aluminum MMCs, in relation to VAWTs. This can be addressed in this study, which will provide essential information on the merits and demerits of using advanced materials in wind turbine construction. Using ANSYS, which is a standard program for FEA, helps make sure that these outcomes are reliable and can support informed decisions about the choice of materials and design optimization for VAWTs.

3. Results Analysis

Finite element analysis (FEA) was used to examine mode shapes and their corresponding natural frequencies for aluminum-constructed VAWT.

3.1. Mode Shapes and Natural Frequencies Analysis for Aluminum VAWT

From the FEA analysis of VAWT made of aluminum, the first mode shape is obtained. The first mode shape obtained from the analysis is of the transverse type along the vertical

direction, as shown in Figure 5. The maximum deformation obtained from the analysis is 12.926 mm, which is observed for vertical vanes.

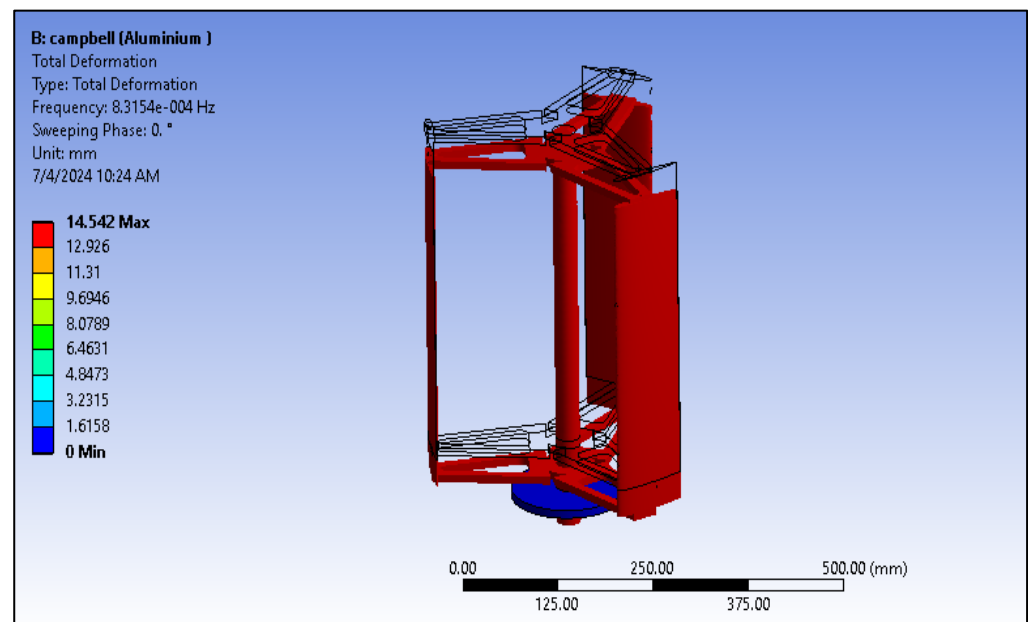


Figure 5. Mode shape of first natural frequency for Aluminum VAWT.

The second mode shape obtained from the analysis is of the torsional type. The maximum deformation obtained from the analysis is 17.07 mm, which is observed for vertical vanes, as represented by red colored zone. The deformation of the center shaft is minimal, as represented by a dark blue colored zone in Figure 6.

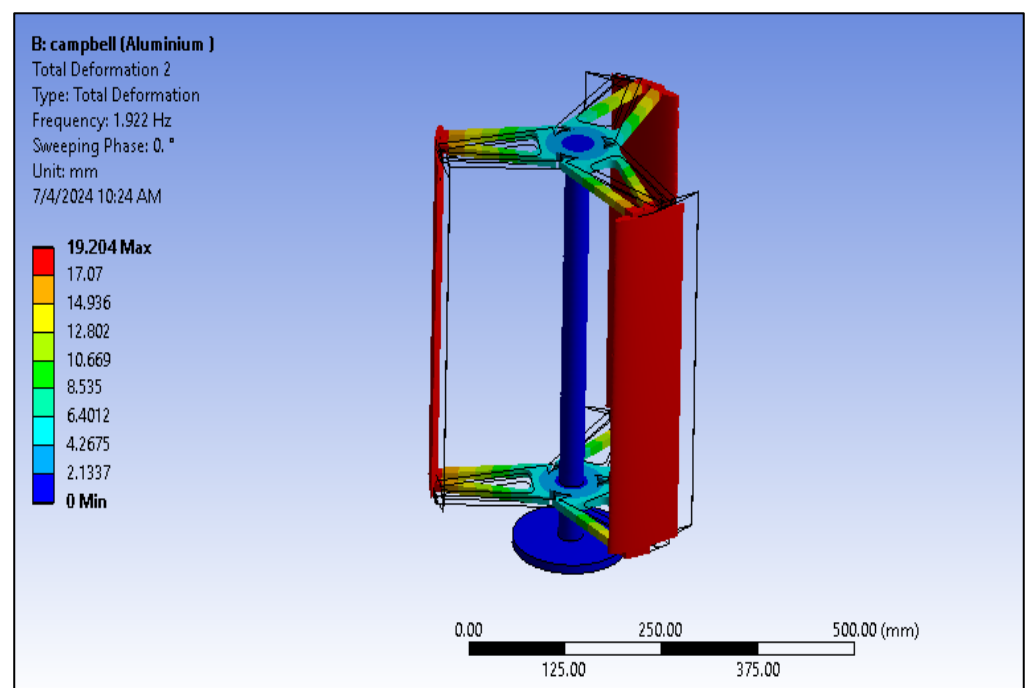


Figure 6. Mode shape of second natural frequency for aluminum VAWT.

The third mode shape, combining both torsional and transverse characteristics, shows a maximum deformation of 20.85 mm, primarily in the vertical vanes as, represented by the red-colored zone in Figure 7. The undeformed model of VAWT is shown in the

wireframe. This pattern continues in the fourth and fifth mode shapes, where the maximum deformations are 20.805 mm and 17.05 mm, respectively.

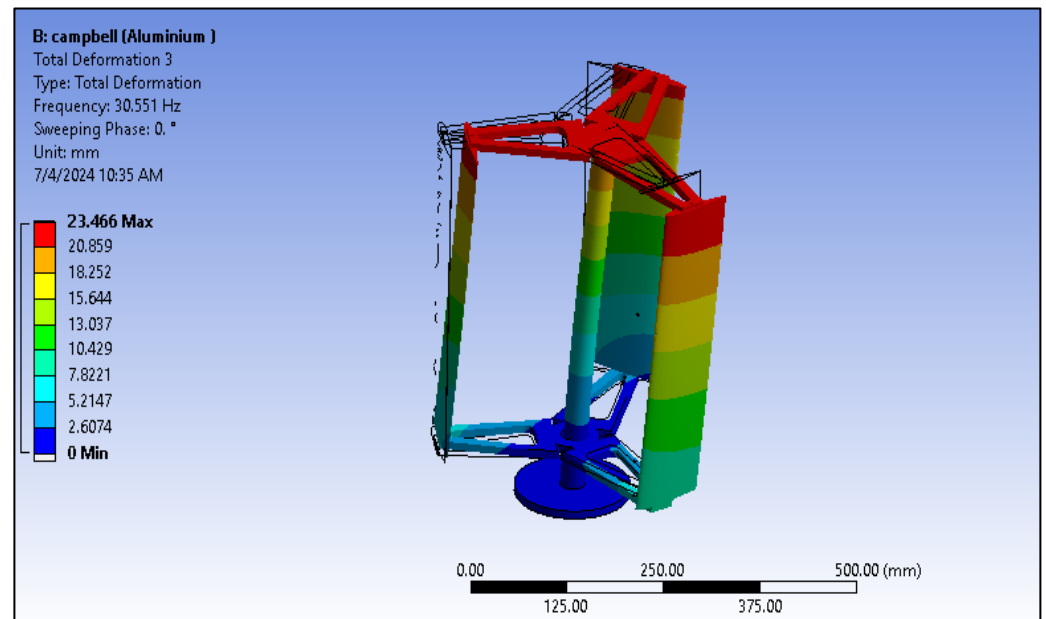


Figure 7. Mode shapes of third natural frequencies for aluminum VAWT.

The fourth mode shape obtained from the analysis is of the transverse type. The maximum deformation obtained from the analysis is 20.80 mm, which is observed for vertical vanes, as represented by red colored zone in Figure 8. The deformation of the center shaft is minimal as represented by a dark blue colored zone. The undeformed model of VAWT is shown in the wireframe.

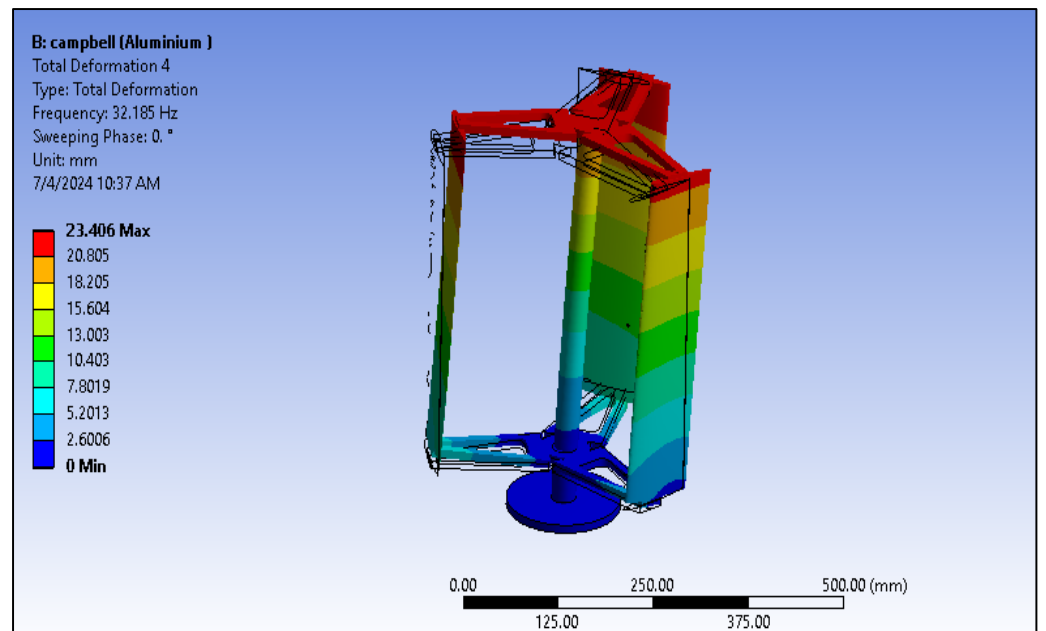


Figure 8. Mode shape of fourth natural frequency.

The fifth mode shape obtained from the analysis is of the transverse type. The maximum deformation obtained from the analysis is 17.05 mm, which is observed for vertical vanes, as represented by red colored zone. The deformation of the center shaft is minimal,

as represented by a dark blue colored zone in Figure 9. The undeformed model of VAWT is shown in the wireframe.

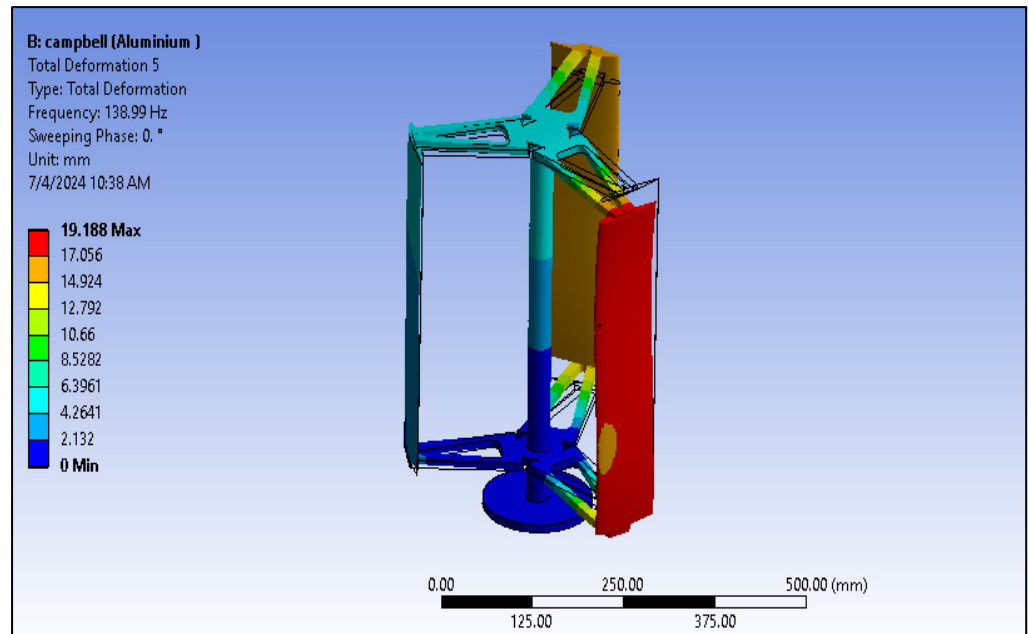


Figure 9. Mode shape of fifth natural frequency.

3.2. Campbell Diagram Analysis for Aluminum VAWT

The Campbell diagram for the aluminum VAWT in Figure 10 reveals that Mode 1 remains undetermined and stable, likely a rigid body mode with a low natural frequency. Modes 2, 3, and 6 exhibit stable backward whirl (BW) across the rotational velocity range. Similarly, Modes 4 and 5 show stable forward whirl (FW), with no significant change in frequency as the rotational speed increases. Notably, no critical speeds are indicated, suggesting that the system operates safely within the range of 17.80 to 48.17 rad/s, without encountering resonance.

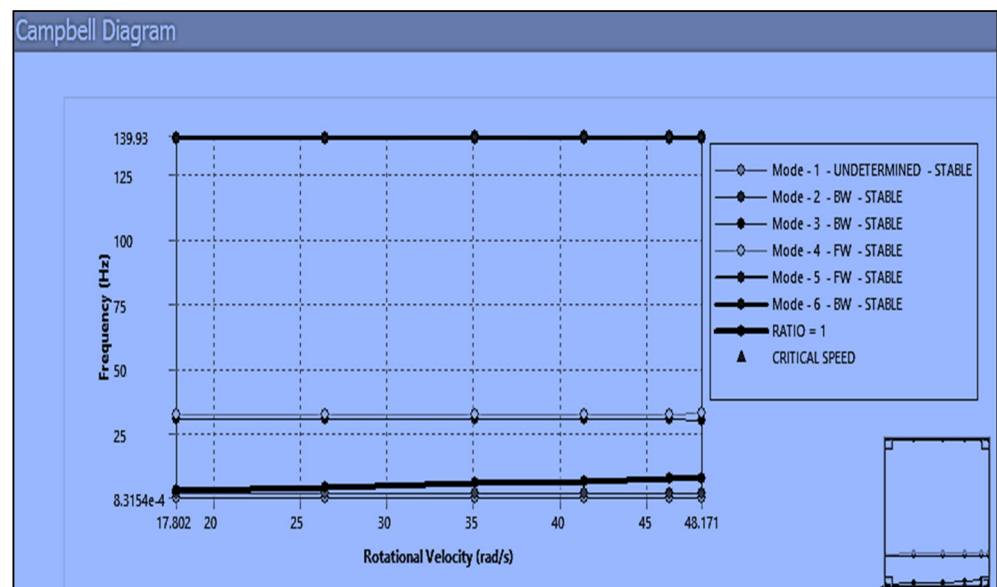


Figure 10. Campbell diagram of aluminum VAWT.

For Al VAWT, Mode 1 is undetermined and stable. This mode remains constant across the entire range of rotational velocities. It is likely a rigid body mode or a mode with a very low natural frequency that does not interact with the rotational speeds considered. Modes 2, 3, and 6 exhibit backward whirl and are stable. These modes also remain relatively constant and stable across the rotational velocity range. They are not influenced by the speed increase, indicating stable backward whirl modes. Modes 4 and 5 exhibit forward whirl and are stable. Similar to the BW modes, these FW modes are stable and do not show a significant change with increasing rotational speed. This indicates forward-whirl modes that are stable. There are no critical speeds (red triangles) indicated on the diagram, suggesting that within the operational range of 17.80 to 48.17 rad/s, the system does not encounter any critical speeds where resonance could occur. The ratio 1 line (black line) represents the first harmonic of the rotor speed. It is used to identify potential resonance conditions if any natural frequencies in the system cross this line. In this diagram, no mode crosses the ratio 1 line, indicating that the natural frequencies of the system do not match the rotational frequency, avoiding potential resonance issues. The system exhibits overall stability across the operational range of rotational speeds. No modes show instability or significant frequency variation. Since there are no crossings of the critical speed line, the system is safe to operate within the specified range of rotational speeds without encountering resonance-induced failures. Regular monitoring of the system is necessary to ensure that the stability observed in the Campbell diagram persists during actual operation. If the operational range of the VAWT is extended beyond the current limits (48.171 rad/s), further analysis should be conducted to ensure stability at higher speeds. This analysis suggests that the VAWT design is robust within the tested rotational velocity range, with no immediate concerns for resonant conditions that could lead to mechanical failure.

3.3. Boron Al MMC VAWT Mode Shapes and Natural Frequencies

For the VAWT constructed from boron Al MMC, the first mode shape is also transverse, with a maximum deformation of 13.09 mm observed in the vertical vanes (Figure 11). The subsequent mode shapes show maximum deformations of 17.28 mm, 21.39 mm, 21.31 mm, and 20.41 mm for the second, third, fourth, and fifth modes, respectively, all primarily affecting the vertical vanes.

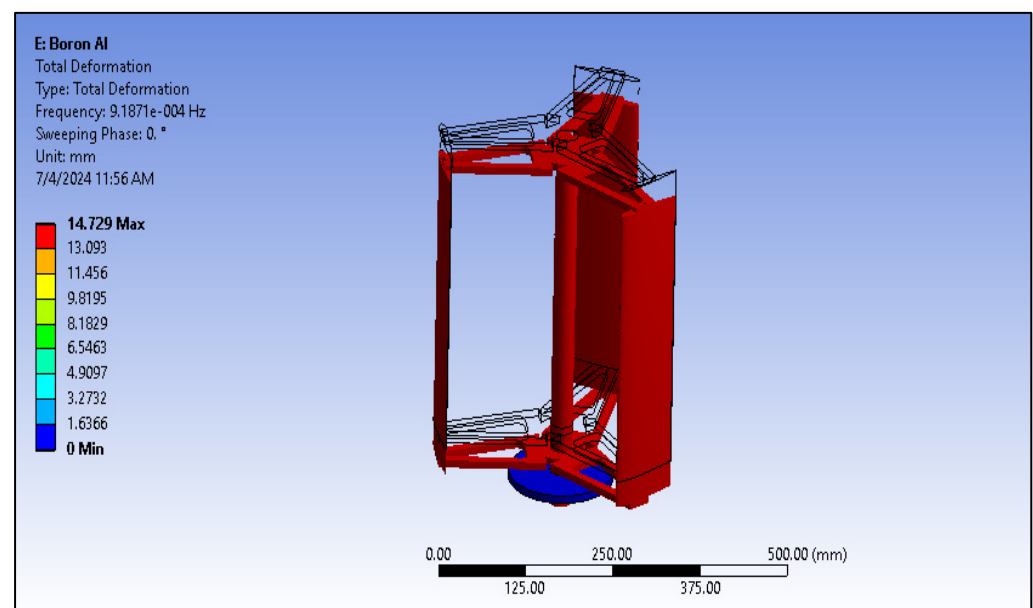


Figure 11. Mode shape of first natural frequency for boron Al.

From the FEA analysis of VAWT made of boron Al, the first mode shape is obtained as shown in Figure 11. The first mode shape obtained from the analysis is of the transverse type along the vertical direction. The maximum deformation obtained from the analysis is 13.03 mm, which is observed for vertical vanes.

From the FEA analysis of VAWT made of boron Al, the second mode shape is obtained as shown in Figure 12. The second mode shape obtained from the analysis is of the transverse type along the vertical direction. The maximum deformation obtained from the analysis is 17.28 mm, which is observed for vertical vanes.

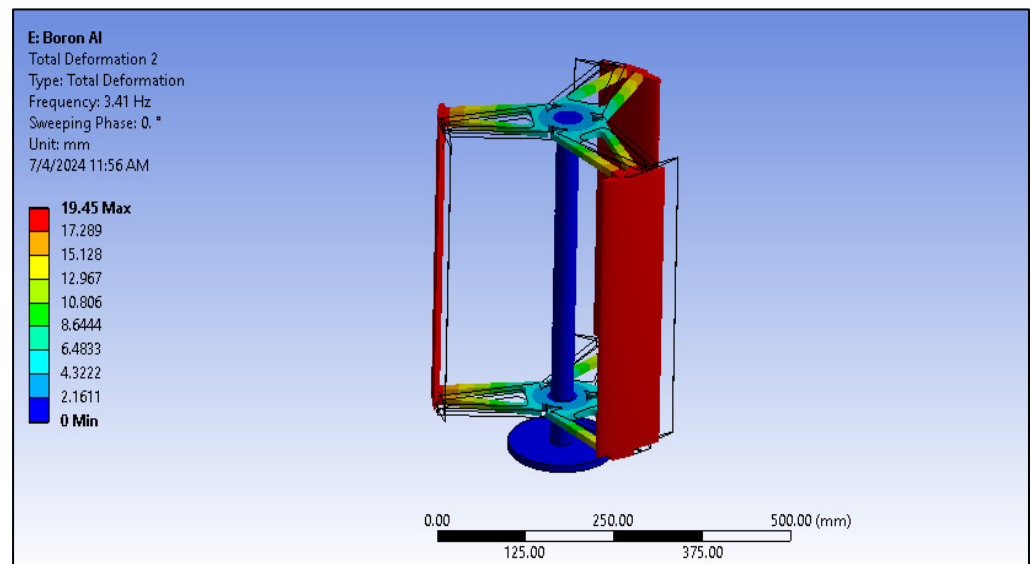


Figure 12. Mode shape of second natural frequency for boron Al.

From the FEA analysis of VAWT made of boron Al, the third mode shape is obtained in Figure 13. The third mode shape obtained from the analysis is of the transverse type along the vertical direction. The maximum deformation obtained from the analysis is 21.39 mm, which is observed for vertical vanes.

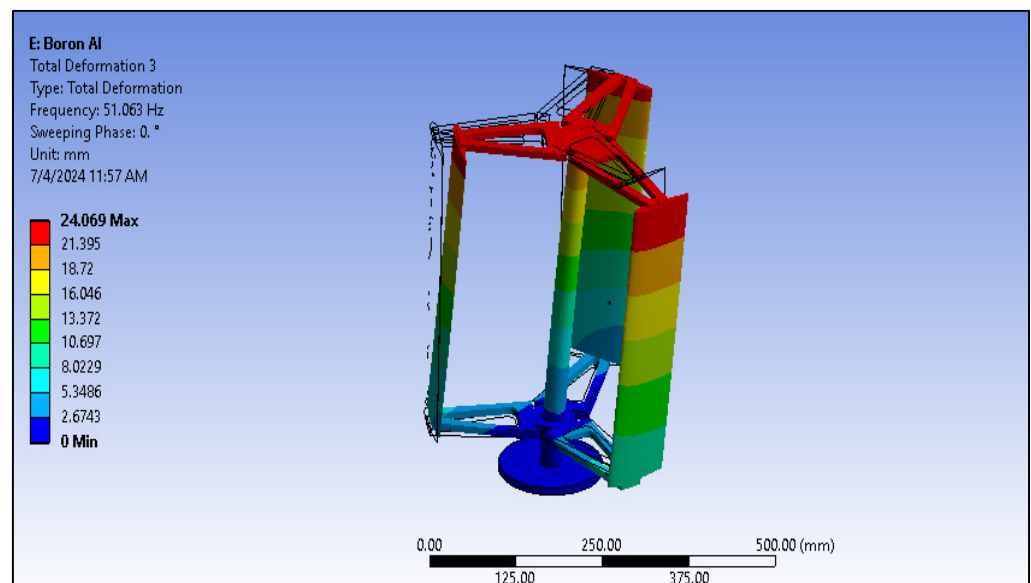


Figure 13. Mode shape of third natural frequency for boron Al.

From the FEA analysis of VAWT made of boron Al, the fourth mode shape is obtained as shown in Figure 14. The fourth mode shape obtained from the analysis is of the transverse

type along the vertical direction. The maximum deformation obtained from the analysis is 21.31 mm, which is observed for vertical vanes.

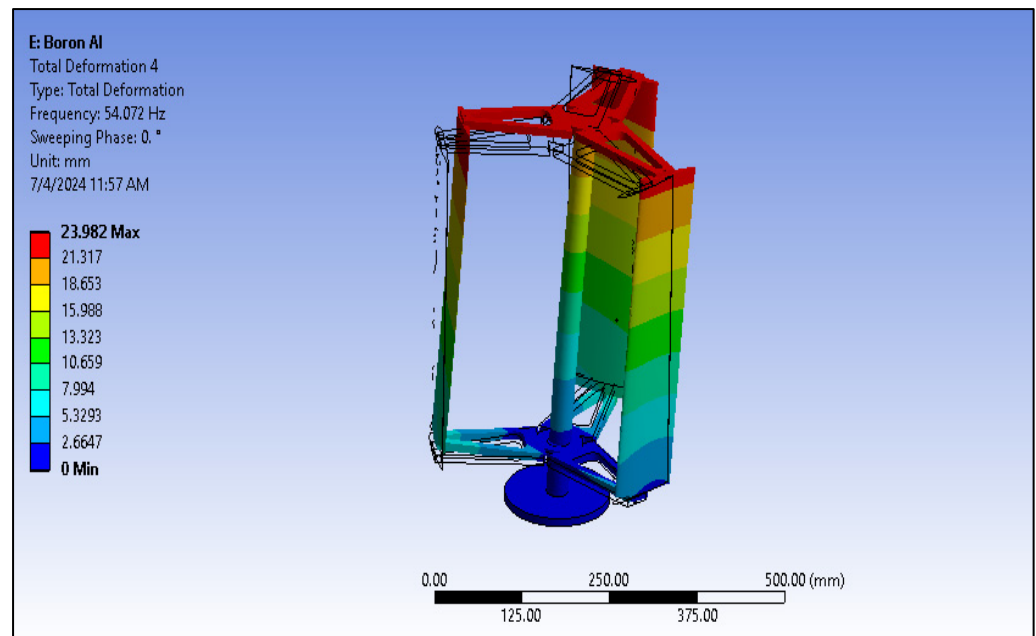


Figure 14. Mode shape of fourth natural frequency for boron Al.

From the FEA analysis of the VAWT made of boron Al, the fifth mode shape is obtained as shown in Figure 15. The fifth mode shape obtained from the analysis is of the torsional type. The maximum deformation obtained from the analysis is 20.41 mm, which is observed for vertical vanes.

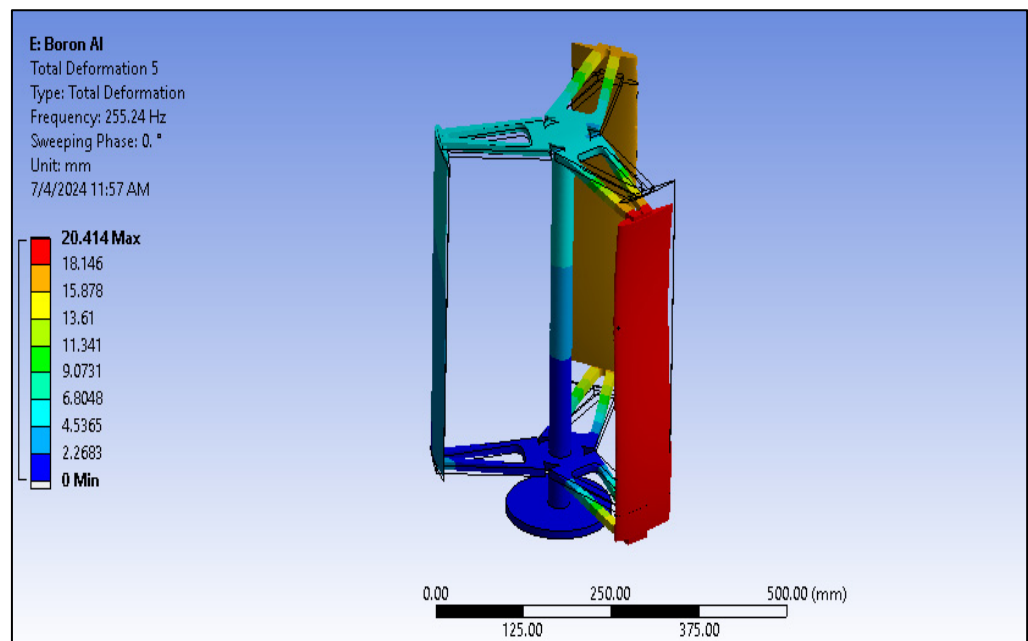


Figure 15. Mode shape of fifth natural frequency for boron Al.

3.4. Campbell Diagram Analysis for Boron Aluminum VAWT

The Campbell diagram in Figure 16 for the boron Al VAWT shows similar stability patterns for Modes 1, 2, 3, and 6 as for the aluminum VAWT, with stable BW and FW modes. However, a critical speed is observed at approximately 20 rad/s, where one of

the system's natural frequencies intersects the rotational speed, indicating a potential resonance condition.

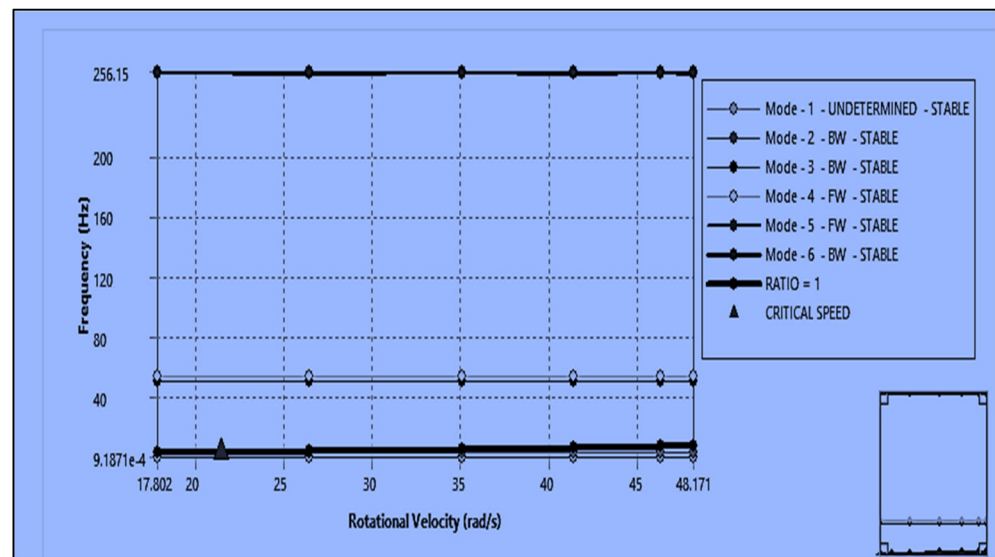


Figure 16. Campbell diagram for boron AI VAWT.

For boron AI VAWT, Mode 1 (Undetermined—Stable): Similar to the previous diagram, Mode 1 remains stable and undetermined across the rotational velocities. Modes 2, 3, and 6 (BW, Backward Whirl—Stable): These modes remain constant and stable across the entire range of rotational velocities, indicating stable backward whirl modes. Modes 4 and 5 (FW, Forward Whirl—Stable): These forward whirl modes are also stable, showing no significant change with increasing rotational speed. The critical speed is indicated by the red triangle and occurs at approximately 20 rad/s. This is a critical point where one of the system's natural frequencies matches the rotational speed, potentially leading to resonance. The corresponding frequency at this critical speed is slightly above 9.18 Hz, as shown on the vertical axis. The ratio 1 line (black line) represents the first harmonic of the rotor speed. It is used to identify potential resonance conditions. Only one mode (possibly Mode 4: FW, red line) crosses the ratio 1 line at the critical speed, suggesting a potential resonance condition at around 20 rad/s. The system exhibits overall stability across most of the operational range of rotational speeds, except at the identified critical speed. The critical speed of approximately 20 rad/s needs careful consideration. Operating near this speed can lead to resonance, which may cause mechanical failures or increased vibrations. To ensure safety and stability, it is advisable to avoid operating the system near the critical speed of 20 rad/s. Consider implementing damping mechanisms to mitigate the effects of resonance at the critical speed. If the operational range needs to be extended beyond the current limits, further analysis should be conducted to ensure stability at higher speeds. The critical speed of the system is around 20 rad/s, with a corresponding frequency of slightly above 9.18 Hz. Modes are stable across the entire range, but the system should avoid the critical speed to prevent resonance-induced issues.

3.5. The Mass Participation Factor

The mass participation factor obtained for aluminum VAWT shows that the first mode shape is the most significant; it contributes to the highest mass participation (mass participation factor of 2.17), as shown in Table 3.

Table 3. Mass participation factor using aluminum.

Mode	Frequency (Hz)	Period (s)	Partic. Factor	Ratio	Effective Mass	Cumulative Mass Fraction	Ratio of Effective Mass to Total Mass
1	1.18658×10^{-2}	842.76	2.1744	1	4.72818	1.00000	0.781224
2	1.78083	0.56154	-2.8646×10^{-7}	0	8.20612×10^{-14}	1.00000	1.35587×10^{-14}
3	28.9986	0.34484	5.6598×10^{-5}	0.000026	3.20330×10^{-8}	1.00000	5.29273×10^{-9}
4	35.6893	0.2802	1.1727×10^{-3}	0.000054	1.37515×10^{-7}	1.00000	2.27213×10^{-8}
5	137.51	0.72722×10^{-2}	-7.0331×10^{-6}	0.000003	4.94649×10^{-10}	1.00000	8.17294×10^{-11}
6	142.463	0.70193×10^{-2}	1.9680×10^{-4}	0.000009	3.87294×10^{-9}	1.00000	6.39915×10^{-10}
Sum					4.72818		0.781224

The ratio of effective mass value suggests that Mode 1 captures approximately 78.12% of the total mass participation in the Z direction.

The mass participation factor obtained for boron VAWT in Table 4 shows that the first mode shape is the most significant; it contributes to the highest mass participation (mass participation factor of 0.067). The ratio of effective mass value suggests that Mode 1 captures approximately 91% of the total mass participation in the Z direction.

Table 4. Mass participation factor using boron/Al.

Mode	Frequency (Hz)	Period (s)	Partic. Factor	Ratio	Effective Mass	Cumulative Mass Fraction	Ratio of Effective Mass to Total Mass
1	9.18708×10^{-4}	1.0885×10^3	6.7892×10^{-1}	1	4.60934×10^{-2}	1.00000	0.91008
2	3.40999	2.9326×10^{-1}	-4.3542×10^{-7}	6.00000×10^{-6}	1.89591×10^{-12}	1.00000	3.74333×10^{-10}
3	51.0629	1.9584×10^{-1}	-1.6833×10^{-8}	0	2.83333×10^{-15}	1.00000	5.59420×10^{-13}
4	54.072	1.8494×10^{-1}	-1.3298×10^{-8}	0	1.76835×10^{-15}	1.00000	3.49148×10^{-13}
5	255.239	3.9179×10^{-2}	7.0566×10^{-8}	0	4.97960×10^{-16}	1.00000	9.83185×10^{-14}
6	255.739	3.9102×10^{-2}	-6.1268×10^{-7}	1.00000×10^{-6}	3.75380×10^{-14}	1.00000	7.41160×10^{-12}
Sum					4.60934×10^{-2}		0.91008

3.6. Deformation and Equivalent Stress Analysis

The deformation induced on Al VAWT is 0.38 mm, as represented by a red-colored zone, and reaches its maximum at the mid-section of the airfoil, as shown in Figure 17. This deformation is lower on the other end of the airfoil. The maximum equivalent stress induced on Al VAWT is 56.42 MPa at the corners where the stress concentration occurs, as shown in Figure 18.

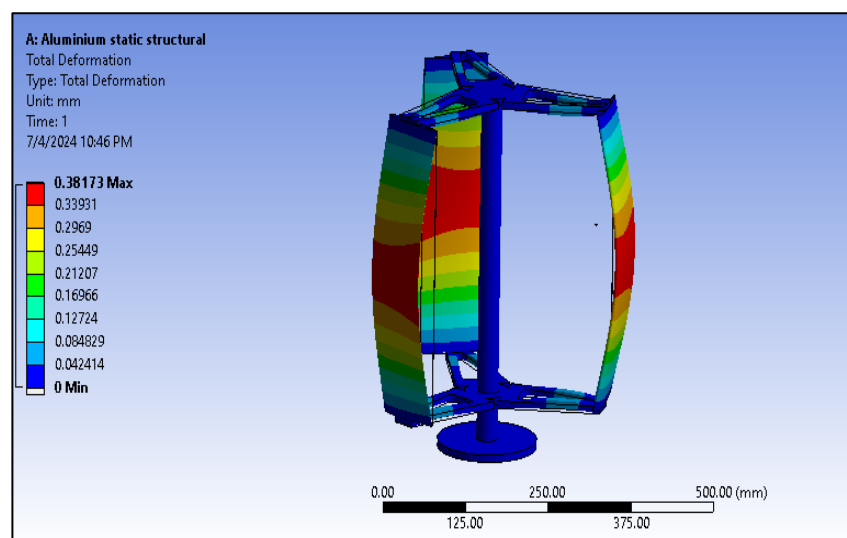


Figure 17. Total deformation on Al VAWT.

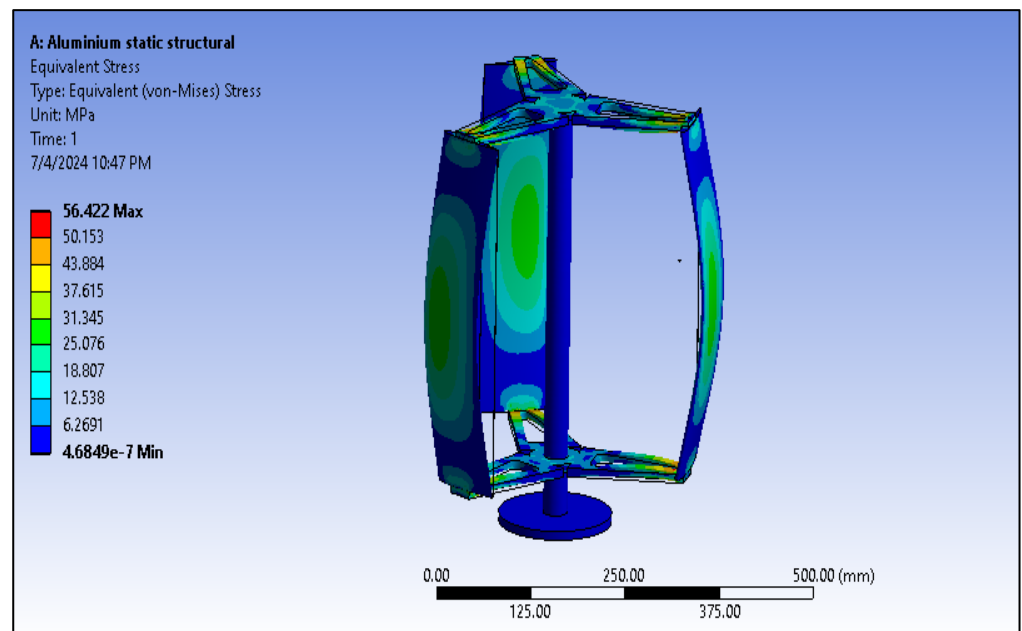


Figure 18. Equivalent stress plot on Al VAWT.

The deformation induced on boron Al VAWT is 0.11 mm, as represented by a red-colored zone, and reaches its maximum at the mid-section of the airfoil, as shown in Figure 19.

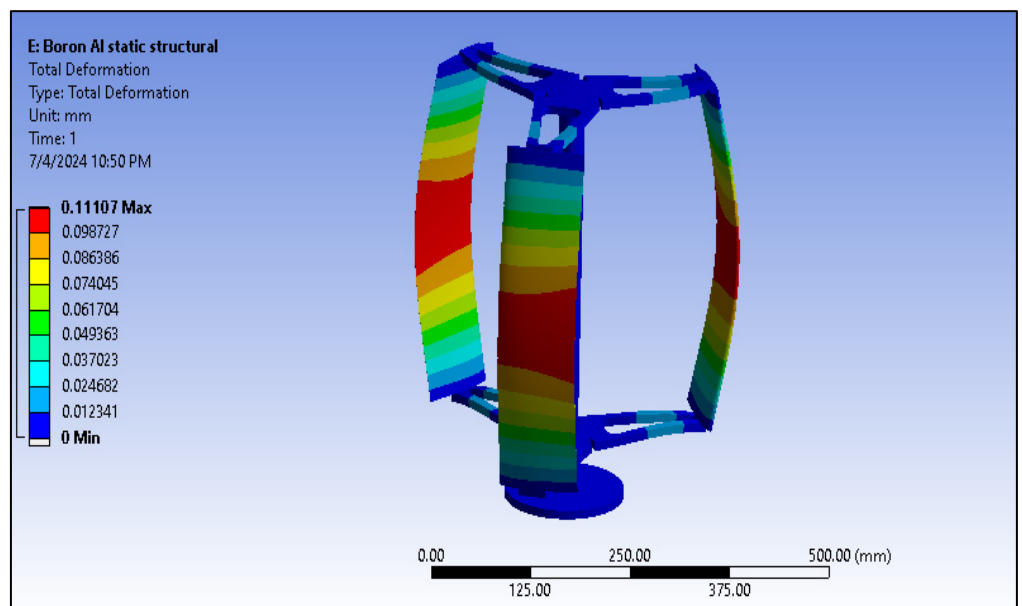


Figure 19. Total deformation on boron Al VAWT.

This deformation is lower on the other end of the airfoil. The maximum equivalent stress induced on Al VAWT is 19.31 MPa at the corners wherein the stress concentration occurs as shown in Figure 20.

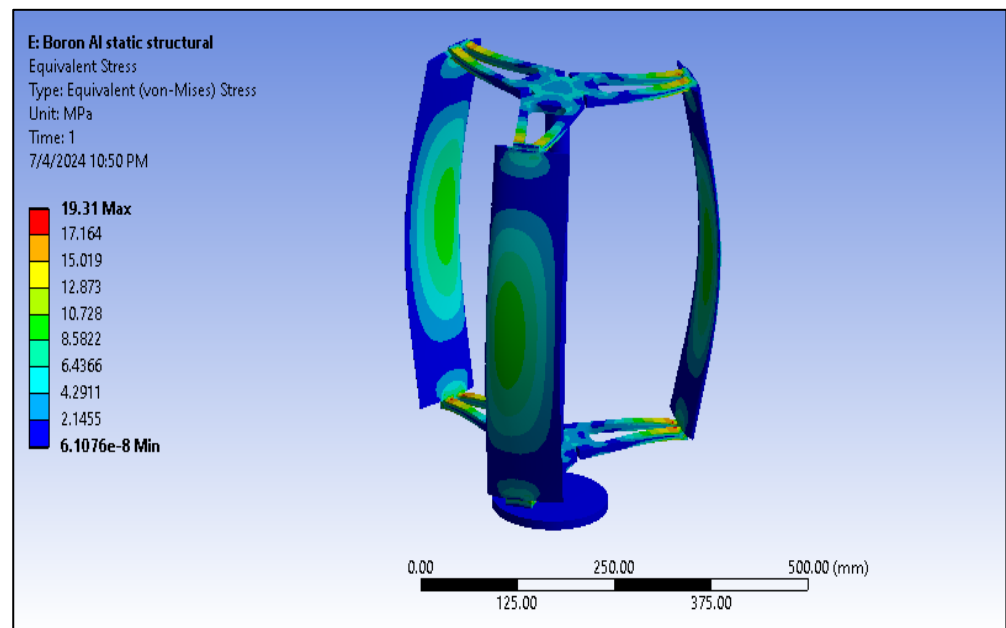


Figure 20. Equivalent stress on boron Al VAWT.

The static structural analysis in Table 5 reveals significant differences between the aluminum and boron Al VAWTs. The maximum deformation in the aluminum VAWT is 0.381 mm (Figure 17), while in the boron Al VAWT, it is 0.11 mm (Figure 19). The maximum equivalent stress in the aluminum VAWT is 56.42 MPa (Figure 18), compared to 19.31 MPa in the boron Al VAWT (Figure 20).

Table 5. Static structural analysis results.

Material Type	Aluminum Alloy	Boron Al MMC
Equivalent stress (MPa)	56.42	19.31
Deformation (mm)	0.38	0.11

3.7. Grid Independence Evaluation and Validation

The grid independence analysis (Table 5) was carried out to validate the finite element analysis results used in this work. Different meshes in several categories were examined, starting with 93,245 to 94,247 elements with the equivalent stresses of the points at the critical section of the VAWT model. The figures also seem to show equivalent stress values that are very much uniform across nodes, thus showing mesh independence. In particular, a small variation was detected for the number of elements ranging from 93,245 to 94,247, in which the equivalent stress rose from 54.11 MPa to 56.42. Their values are quite close and average at 422 MPa. This validates the chosen mesh density of 94,247 elements, through which the numerical error is close to zero and above, hence the correctness of stress predictions when conducting structural analysis of VAWTs using boron Al MMC. The mesh-independent study results are shown in Table 6.

Table 6. Grid independence chart.

Number of Elements	Equivalent Stress
93,245	54.111
93,769	54.148
93,988	55.568
94,201	56.421
94,247	56.422

The obtained values of equivalent stress are in good agreement with the previously conducted experimental investigation in [28], with a 4.2% deviation, which is considered acceptable. The equivalent stress, according to the literature, is 54.1 Mpa, and the von Mises stress calculated from the same FEA analysis is 56.42 Mpa, and this is near the acceptance level. This comparison has helped to increase confidence in the results generated via FEA, and hence their reliability and accuracy. Hence, these findings are considered significant and can be used to inform future decision-making regarding choosing materials, redesigning configurations, and determining strategies for structural applications similar to this one.

4. Discussion

The boron Al MMC demonstrates superior performance compared to the aluminum alloy in terms of both stress and deformation. The equivalent stress in the boron Al MMC is approximately 65.77% lower, and the deformation is about 70.92% lower, than that of aluminum. These results suggest that boron Al MMC can endure higher loads with minimal stress and deformation, enhancing the VAWT's structural integrity and operational longevity. This analysis indicates that using boron Al MMC could significantly improve the reliability and durability of VAWTs, making it a viable material choice for future turbine designs.

Campbell plots further confirm these results; both materials remain stable for the range of rotational speeds studied. A significantly lower critical speed is highlighted in the boron Al VAWT. This would need to be monitored, with potential design changes made for the avoidance of failure from resonance.

Accordingly, as indicated by the mass participation factor results, the higher mass participation factor of about 91% of the boron Al VAWT's Mode 1 for the Z direction is reasonable for higher materials like boron Al MMC. This was expected because the boron Al MMC possesses higher values of modulus of elasticity and damping capacity than those of conventional aluminum alloys. Thus, the great variety of mass performances indicates that it is possible to eliminate vibrations and resonance problems by using boron Al MMC, which, in turn, will improve the dynamic characteristics of VAWTs. Also, the boron Al has higher durability and longevity, which causes higher operational life. It has higher long-term savings and lower maintenance requirements. These recommendations are relevant and therefore justified as they stem from the research hypothesis that, compared to aluminum, boron Al MMC would offer superior dynamic characteristics. Thus, these expected results demonstrate that advanced materials such as boron Al MMC have much to offer VAWT technology over conventional materials.

5. Conclusions

This study was intended to examine the dynamic and static efficiencies of VAWTs made of aluminum alloy and boron Al MMC in answering certain research hypotheses and questions regarding renewable energy technologies. The results of the dynamic, as well as the static, analysis prove the appropriateness of using boron Al MMC material, identifying several advantages of using it instead of the aluminum alloy. Our research hypothesis entails the proposition that the incorporation of boron Al MMC into the fabrication of a VAWT blade would improve its dynamic performance over that made of the aluminum alloy. These analyses supported our hypothesis, demonstrating that boron Al MMC VAWTs have higher natural frequencies and better mode shapes, which are essential in minimizing vibrations and increasing operational stability. The static structural analysis further revealed that boron Al MMC has better mechanical characteristics because of its high stiffness and because of its lesser equivalent stress of 65.77% are lower deformation of 70.92% compared to that of the aluminum alloy under operational loads.

In addressing the research questions, it was possible to distinguish the dynamic characteristics indicating that aluminum alloy and boron Al MMC VAWTs exhibit crucial differences. Investigations of aluminum alloy VAWTs pointed towards stable natural frequencies and mode shapes of the turbine blade, and no critical speeds were noted, which emphasizes that the turbine can operate under standard operational conditions with reliability. On the other hand, Boron-Al MMC VAWTs exhibit similar stability. However, a critical speed of around 20 rad/s was observed, which makes these VAWTs susceptible to resonance issues. Therefore, proper consideration of damped control is required to enhance stability. Thus, this study also looked in more detail into using boron Al MMC in VAWTs. On the positive side, the material provides increased mechanical strength and long-term durability, but the presence of the critical speed raises questions that should be answered in order to provide safe and reliable rotary equipment operation for the years to come.

These findings reinforce the need for material science engineering to be applied with VAWT design to achieve its optimum performance and durability in the renewable energy sector. Hence, these results confirm the working hypothesis of this study, proving the expected improvements in dynamic performance variables with the boron Al MMC. Secondly, the material demonstrated good damping capability and potential for self-support of the structure under various loads, which may help increase efficiency and extend the lifespan of VAWTs. Given these developments, this study also acknowledges the limitations of simulated analyses and the requirement for further experimental validation in real life to improve reliability and relevance.

Future research directions could focus on refining damping strategies, validating findings through field tests, addressing economic aspects, and optimizing manufacturing processes to overcome challenges related to the practical deployment of MMCs in renewable energy technologies. The current research provides new and original insights related to material selection for VAWTs and helps to put forward the potential of boron Al MMC in sustainable and efficient renewable energy technologies.

Author Contributions: Conceptualization, A.A. and L.M.; methodology, A.A.; software, A.A.; validation, A.A. and L.M.; formal analysis, A.A.; investigation, A.A. and L.M.; resources, L.M.; data curation, A.A.; writing—original draft preparation, A.A.; writing—review and editing, A.A. and L.M.; visualization, A.A. and L.M.; project administration, A.A. and L.M.; funding acquisition, L.M. All authors have read and agreed to the published version of the manuscript.

Funding: This research received no external funding.

Data Availability Statement: Data are contained within the article.

Conflicts of Interest: The authors declare no conflicts of interest.

References

1. Kalmikov, A. Wind Power Fundamentals. In *Wind Energy Engineering*; Elsevier: Amsterdam, The Netherlands, 2023; pp. 23–27.
2. Gennitsaris, S.; Sofianopoulou, S. Wind Turbine End-of-Life Options Based on the UN Sustainable Development Goals (SDGs). *Green Technol. Sustain.* **2024**, *2*, 100108. [[CrossRef](#)]
3. Ghorani, M.M.; Karimi, B.; Mirghavami, S.M.; Saboohi, Z. A Numerical Study on the Feasibility of Electricity Production Using an Optimized Wind Delivery System (Invelox) Integrated with a Horizontal Axis Wind Turbine (HAWT). *Energy* **2023**, *268*, 126643. [[CrossRef](#)]
4. Sinha, P.; Agarwal, A.; Rejeesh, C.R. Computational Fluid Dynamics Analysis of the Influence of Openings on Wind Load and Structural Response in Triangular Buildings. *J. Sustain. Energy* **2023**, *2*, 50–67. [[CrossRef](#)]
5. Han, Z.; Chen, H.; Chen, Y.; Su, J.; Zhou, D.; Zhu, H.; Xia, T.; Tu, J. Aerodynamic Performance Optimization of Vertical Axis Wind Turbine with Straight Blades Based on Synergic Control of Pitch and Flap. *Sustain. Energy Technol. Assess.* **2023**, *57*, 103250. [[CrossRef](#)]
6. Kaewbumrung, M.; Plengsa-Ard, C.; Pansang, S.; Palasai, W. Preventive Maintenance of Horizontal Wind Turbines via Computational Fluid Dynamics-Driven Wall Shear Stress Evaluation. *Results Eng.* **2024**, *22*, 102383. [[CrossRef](#)]
7. Agarwal, A.; Letsatsi, M.T.; Pitso, I. Thermodynamic Analysis of Wind Catcher with Cooling Pads Using SSG Reynolds Stress Turbulence Model. *J. Eng. Res.* **2021**, 1–13. [[CrossRef](#)]

8. Agarwal, A.; Mthembu, L. Structural Analysis and Optimization of Heavy Vehicle Chassis Using Aluminium P100/6061 Al and Al GA 7-230 MMC. *Processes* **2022**, *10*, 320. [[CrossRef](#)]
9. Cheng, B.; Yao, Y.; Qu, X.; Zhou, Z.; Wei, J.; Liang, E.; Zhang, C.; Kang, H.; Wang, H. Multi-Objective Parameter Optimization of Large-Scale Offshore Wind Turbine's Tower Based on Data-Driven Model with Deep Learning and Machine Learning Methods. *Energy* **2024**, *305*, 132257. [[CrossRef](#)]
10. Soufyane, B.; Abdelhamid, R.; Smail, Z.; Elhafyani, M.L.; Hajjaji, A. El Fully Robust Sensorless Control of Direct-Drive PMSG Wind Turbine Feeding a Water Pumping System. *IFAC-Pap.* **2020**, *53*, 12797–12802. [[CrossRef](#)]
11. Barnes, A.; Hughes, B. Determining the Impact of VAWT Farm Configurations on Power Output. *Renew. Energy* **2019**, *143*, 1111–1120. [[CrossRef](#)]
12. Machado, M.R.; Dutkiewicz, M. Wind Turbine Vibration Management: An Integrated Analysis of Existing Solutions, Products, and Open-Source Developments. *Energy Rep.* **2024**, *11*, 3756–3791. [[CrossRef](#)]
13. Linda, M.; Agarwal, A.; Sinha, P. Computational Fluid Dynamics Analysis of Vertical Axis Wind Turbine Heights for Enhanced Hydrogen Production in Urban Environments. *J. Intell. Syst. Control* **2023**, *2*, 123–131. [[CrossRef](#)]
14. Dinh, V.-N.; Basu, B. Passive Control of Floating Offshore Wind Turbine Nacelle and Spar Vibrations by Multiple Tuned Mass Dampers. *Struct. Control Health Monit.* **2015**, *22*, 152–176. [[CrossRef](#)]
15. Agarwal, A. Computational Investigation of Vertical Axis Wind Turbine in Hydrogen Gas Generation Using PEM Electrolysis. *J. New Mater. Electrochem. Syst.* **2022**, *25*, 172–178. [[CrossRef](#)]
16. Brodersen, M.L.; Bjørke, A.-S.; Høgsberg, J. Active Tuned Mass Damper for Damping of Offshore Wind Turbine Vibrations. *Wind Energy* **2017**, *20*, 783–796. [[CrossRef](#)]
17. Coudurier, C.; Lepreux, O.; Petit, N. Passive and Semi-Active Control of an Offshore Floating Wind Turbine Using a Tuned Liquid Column Damper. *IFAC-Pap.* **2015**, *48*, 241–247. [[CrossRef](#)]
18. Van der Woude, C.; Narasimhan, S. A Study on Vibration Isolation for Wind Turbine Structures. *Eng. Struct.* **2014**, *60*, 223–234. [[CrossRef](#)]
19. Ismail, M.; Ikhrouane, F.; Rodellar, J. The Hysteresis Bouc-Wen Model, a Survey. *Arch. Comput. Methods Eng.* **2009**, *16*, 161–188. [[CrossRef](#)]
20. Geng, F.; Suiker, A.S.J.; Rezaeiha, A.; Montazeri, H.; Blocken, B. A Computational Framework for the Lifetime Prediction of Vertical-Axis Wind Turbines: CFD Simulations and High-Cycle Fatigue Modeling. *Int. J. Solids Struct.* **2023**, *284*, 112504. [[CrossRef](#)]
21. Fang, W.; Jia, Z.; Xiao, J.; Sun, C.; Li, L.; Chao, F. A Self-Coupling Proportion Differential Control Method for Vibration Suppression-Based Wind Turbine System. *Sustain. Energy Technol. Assess.* **2024**, *68*, 103831. [[CrossRef](#)]
22. Narasinh, V.; Mital, P.; Chakravorty, N.; Mittal, S.; Kulkarni, N.; Venkatraman, C.; Geetha Rajakumar, A.; Banerjee, K. Investigating Power Loss in a Wind Turbine Using Real-Time Vibration Signature. *Eng. Fail. Anal.* **2024**, *159*, 108010. [[CrossRef](#)]
23. Zhang, J.; Liang, X.; Wang, B.; You, P.; Yun, L. Vibration Reduction and Energy Harvesting of Monopile Offshore Wind Turbines under Extreme Wind-Wave Loadings Using a Novel Bidirectional Absorber-Harvester. *Structures* **2024**, *66*, 106790. [[CrossRef](#)]
24. Castellani, F.; Natili, F.; Astolfi, D.; Vidal, Y. Wind Turbine Gearbox Condition Monitoring through the Sequential Analysis of Industrial SCADA and Vibration Data. *Energy Rep.* **2024**, *12*, 750–761. [[CrossRef](#)]
25. Dai, Y.; Zhong, L.; Li, B.; Deng, Z.; Wang, J.; He, Z. Study on the Vibration Characteristics of Wind Turbine by Fused Blade Tip Structure. *Ocean Eng.* **2024**, *305*, 117869. [[CrossRef](#)]
26. Xue, P.; Wan, Y.; Takahashi, J.; Akimoto, H. Structural Optimization Using a Genetic Algorithm Aiming for the Minimum Mass of Vertical Axis Wind Turbines Using Composite Materials. *Heliyon* **2024**, *10*, e33185. [[CrossRef](#)]
27. Agarwal, A.; Mthembu, L. Finite Element Investigation of the Vibration Characteristics of Francis Turbine Vanes. In *Emerging Trends in Mechanical and Industrial Engineering: Select Proceedings of ICETMIE 2022*; Springer Nature: Singapore, 2023; pp. 945–960.
28. Hamdan, A.; Mustapha, F.; Ahmad, K.A.; Mohd Rafie, A.S. A Review on the Micro Energy Harvester in Structural Health Monitoring (SHM) of Biocomposite Material for Vertical Axis Wind Turbine (VAWT) System: A Malaysia Perspective. *Renew. Sustain. Energy Rev.* **2014**, *35*, 23–30. [[CrossRef](#)]
29. Castro, D.; Pertuz, A.; León-Becerra, J. Mechanical Behavior Analysis of a Vertical Axis Wind Turbine Blade Made with Fique-Epoxy Composite Using FEM. *Procedia Comput. Sci.* **2022**, *203*, 310–317. [[CrossRef](#)]
30. Liu, W.; Yue, X.; Hu, Q.; Song, Y.; Zhu, B.; Chen, X.; Huang, H. Effects of Recrystallization and Element Diffusion Behavior on Interfacial Bonding Quality and Mechanical Properties of Aluminum Laminated Composites. *J. Alloys Compd.* **2024**, *985*, 174045. [[CrossRef](#)]
31. Rakshith Gowda, D.; Bharath, P.; Ranjith, K.; Rishi, J.P.; Shrinivasa, D. Finite Element Analysis of the Flange with Different Fillet Radius in Tubular Wind Tower. *Mater. Today Proc.* **2022**, *68*, 2551–2559. [[CrossRef](#)]
32. Asadi, N.; Arvin, H.; Žur, K.K. Campbell Diagrams, Dynamics and Instability Zones of Graphene-Based Spinning Shafts. *Appl. Math. Model.* **2023**, *121*, 111–133. [[CrossRef](#)]
33. Sunny, K.A.; Kumar, N.M. Vertical Axis Wind Turbine: Aerodynamic Modelling and Its Testing in Wind Tunnel. *Procedia Comput. Sci.* **2016**, *93*, 1017–1023. [[CrossRef](#)]
34. Rawal, S. Metal-Matrix Composites for Space Applications. *JOM J. Miner. Met. Mater. Soc.* **2001**, *53*, 14–17. [[CrossRef](#)]

35. Ilunga, M.; Agarwal, A. A Finite-Element-Analysis-Based Feasibility Study for Optimizing Pantograph Performance Using Aluminum Metal Matrix Composites. *Processes* **2024**, *12*, 445. [[CrossRef](#)]
36. Agarwal, A.; Cavicchioli Batista, R.; Gurung, A. Analyzing the Impact of Bumper Height on Pedestrian Injuries Using Explicit Dynamics. In *Smart Electric and Hybrid Vehicles*; CRC Press: New York, NY, USA, 2024; pp. 57–89.

Disclaimer/Publisher's Note: The statements, opinions and data contained in all publications are solely those of the individual author(s) and contributor(s) and not of MDPI and/or the editor(s). MDPI and/or the editor(s) disclaim responsibility for any injury to people or property resulting from any ideas, methods, instructions or products referred to in the content.